

Spectroscopy of Fluorescein (FITC) Dyed Colloidal Silica Spheres

A. Imhof,^{*,†,‡} M. Megens,[‡] J. J. Engelberts,[†] D. T. N. de Lang,[‡] R. Sprik,[‡] and W. L. Vos[‡]

Van't Hoff Laboratory for Physical and Colloid Chemistry, Utrecht University, Padualaan 8, 3584 CH Utrecht, The Netherlands, and Van der Waals-Zeeman Instituut, Universiteit van Amsterdam, Valckenierstraat 65, 1018 XE Amsterdam, The Netherlands

Received: July 31, 1998; In Final Form: December 6, 1998

We have measured the absorption spectrum, the emission spectrum, the emission lifetime, and the photostability of fluorescein isothiocyanate (FITC) incorporated inside colloidal silica spheres as a function of the dye concentration in the spheres, while minimizing scattering effects. Six batches of stable, monodisperse particles were synthesized with FITC up to high densities of 0.03 M. At dye concentrations above 0.001 M, we observe a large red shift of 10 nm in the absorption and the emission spectra, as well as a strong reduction of the lifetime. At the same time, the photostability of the dye is considerably improved. These effects are caused by an increased energy transfer between the dye molecules as their concentration increases. Several excitation quenching models are examined, namely annihilation quenching, surface quenching, and a fractal distribution of quenchers. None of the models that assume a homogeneous distribution of FITC provide a sufficient explanation of the observed effects. It is suggested that the dye molecules tend to form clusters during the synthesis of the colloidal spheres. It is concluded that colloids with a low dye concentration are useful for photonic applications, whereas high dye concentrations are interesting for optical experiments in colloid science.

1. Introduction

The incorporation of organic dyes into solid matrices is attracting wide interest because of useful applications as laser materials,¹ nonlinear optical materials,² optical memories,³ or light concentrators in solar cells.⁴ Advantages of incorporating dye molecules in solids compared to liquid solutions are the increased photostability and fluorescence yield.⁵ In liquid solutions the quantum efficiencies of most organic dyes are strongly reduced when relatively low dye concentrations of $\sim 10^{-4}$ M are exceeded. This so-called concentration quenching or self-quenching is due to nonradiative energy transfer between the dye molecules.⁶ Solid host materials, on the other hand, isolate the dye molecules from each other, which reduces unwanted energy transfer because the formation of nonfluorescent aggregates or complexes is prevented.

An exciting new possibility is to incorporate dyes in small solid particles instead of bulk solid material,^{7,8} for many reasons. Small particles reveal interesting optical scattering phenomena, especially in combination with interference effects. An important example occurs in photonic crystals, in which the refractive index varies periodically on distances comparable to the wavelength of light.⁹ The goal is to obtain a photonic band gap that will lead to novel quantum optical phenomena such as inhibition of spontaneous emission.¹⁰ Recently, it has been shown that photonic crystals made of colloidal particles have a strong optical interaction.¹¹ In an early study of spontaneous emission in photonic colloidal crystals, the active dye was dissolved in the liquid medium between colloidal particles.¹² Later, it was recognized that this leads to complications due to chemical interactions of the dye with the particle surfaces.^{13,14} Arguably a cleaner way to study photonic effects is to shield the dye by incorporating it inside colloidal particles, e.g. silica

spheres.^{7,8} Therefore, it is crucial to identify the spectroscopic behavior of dye-laced colloids before studying collective photonic effects. A closely related subject that may benefit from dyed colloids is laser action in random media.¹⁵

A different type of interference effects are the morphological resonances of single micron-sized particles. It has been observed that these resonances have very high quality factors, which have large effects on the radiative properties of dyes, including lasing.¹⁶ Indeed, lasing with a very low threshold of 200 nW has recently been demonstrated in silicate microspheres.¹⁷ It should thus be fruitful to dope such spheres with highly efficient dyes, e.g. if short optical pulses are desired. This is a second reason for a spectroscopic study on the behavior of dye in small particles made of silica.

Another interest in dyed particles stems from colloid science. Van Blaaderen et al. synthesized silica colloids with dye incorporated.^{7,8} Such dyed particles have enabled measurements of particle diffusion by fluorescence recovery after photobleaching,¹⁸ and direct imaging of dense colloidal structures by confocal fluorescence microscopy.¹⁹ Nevertheless, several aspects of the incorporation of dye inside colloids remain open questions. It is not clear whether the dye is dispersed homogeneously through the solid matrix of the colloids. Furthermore, in a previous study of dyed particles,²⁰ it was found that the bleaching as a function of time is clearly non-exponential, but no further interpretation could be given. Therefore, a spectroscopic study is expected to give more insight.

In this work, we specifically study the influence of the amount of labeling (the number density of dye molecules in the particle) on the size and stability of the resulting particles, and on their spectroscopic properties: absorption and fluorescence spectra, photostability (bleachability), and fluorescence lifetimes. It is shown that changes in the various spectroscopic properties take place in unison with an increased dye concentration inside the particles. Self-quenching effects, evidenced by a drastic reduc-

[†] Utrecht University.

[‡] Universiteit van Amsterdam.

series consisting of pure FITC dissolved in a 50:50 v/v mixture of DMF and 0.430 M NaOH in water. The molar extinction coefficient of FITC was found to be $3.64 \times 10^6 \text{ M}^{-1} \text{ m}^{-1}$ (at 490 nm) in this mixture. Note that this procedure assumes either that the bond between APS and FITC in samples of dissolved particles dissociates in the basic solution or that it is of little influence to the absorbance. In support of this assumption, we mention that no difference was found between the shape and location of the absorption spectra of the calibration series and of the dissolved silica particles.

D. Absorption and Fluorescence Spectra. Absorption spectra were measured on dilute dispersions in 1 cm glass cuvettes with a Shimadzu Spectronic 200 UV double-beam spectrophotometer, using DMF as a reference. Fluorescence spectra were measured on the undiluted stock dispersions with a Bio-Rad FTS-60A Fourier Transform spectrofluorimeter. The samples were contained in 2.5 cm diameter cylindrical flasks and illuminated by an argon ion laser (Spectra Physics) with light of 458, 476.5, or 488 nm. Fluorescence was detected in backscattering.

E. Fluorescence Lifetimes. Fluorescence decay curves were measured using a time-correlated single-photon counting technique. Pulses from a mode-locked Nd:YAG laser (Spectra Physics 3800, pulse width ≤ 100 ps) were shortened to 5–10 ps in a pulse compressor (Spectra Physics 3595). These pulses were frequency-doubled before synchronously pumping a mode-locked cavity-dumped dye laser (Spectra Physics 3500) that uses Kiton Red in the wavelength range 600–660 nm. The repetition rate of the cavity dumper was 80 kHz. The dye laser pulses were also frequency-doubled, resulting in an excitation beam of <1 ps (FWHM) pulses with a wavelength of 315 nm and a beam diameter of 1 mm at the sample. The beam intensity was always lower than $1 \mu\text{W}$. The sample was placed in the beam at an angle of 45° in order to prevent direct reflections from entering the detector. The fluorescence was detected at an angle of 90° to the exciting beam by a Hamamatsu R3809U Multi-Channel Plate (MCP) detector after filtering with a Schott RG490 cutoff filter to remove residual laser light. The MCP signal was amplified and fed into a constant fraction discriminator (Tennelec TC454), time to amplitude converter (Tennelec TC864), and multi-channel analyzer (MCA). A photodiode monitored the incident beam for triggering the MCA. By adjusting an aperture in front of the MCP, we could maintain a photon count rate of 12 kcounts/s maximum. The temporal resolution of the setup was 60 ps.

For measuring the effect of excitation intensity, a variable intensity filter was placed in front of the second-harmonic generating crystal. In this way, the photodiode would still be able to detect the (unattenuated) signal. Because of the second-harmonic process, the intensity varied quadratically with variation of the attenuation. In order to measure the relative intensity of the excitation pulse, a power meter was placed immediately behind the sample in the impinging beam.

For the depolarization measurements, we placed 10-mm polarizing prisms in front of the sample and between the sample and the MCP and selected polarizations parallel and perpendicular to the incoming beam.

Samples were taken from the stock dispersions and transferred to 0.4-mm-thick glass capillaries (Vitro Dynamics). Decay curves were corrected for a weak long-lived fluorescence from impurities in the glass of the vials.

F. Photostability. To measure the reduction of fluorescence of the silica particles as a function of exposure to exciting radiation (the bleach curve), a circular spot ~ 2 mm in diameter

TABLE 2: Physical Parameters of the Prepared Silica Spheres^a

system	R_{SLS} (nm)	R_{TEM} (nm)	σ (%)	l_{eff} (%)	c (mM)	R_{avg} (nm)
F0	207	184	6.0	—	—	—
F1	208	188	6.1	6.6	0.49	15.0
F2	218	194	6.3	7.6	1.18	11.2
F3	224	197	6.5	9.1	2.70	8.5
F4	237	210	6.2	10.1	6.00	6.5
F5	250	223	6.6	10.0	11.9	5.2
F6	341	305	16	13.0	31.0	3.8

^a R_{SLS} and R_{TEM} are the particle radii determined by static light scattering and transmission electron microscopy, respectively; σ is the polydispersity; l_{eff} is the labeling efficiency; c is the dye concentration inside the particles; and R_{avg} is the average distance between dye molecules inside the particles.

was illuminated by an 0.10-W, 488-nm laser beam in steps of 1-s duration. After each 1-s pulse the exciting intensity was reduced by a factor of 500, after which the fluorescent intensity was measured by a photodiode under an angle of $\sim 160^\circ$ to the exciting beam, and after filtering by a 515-nm long-pass filter. Samples were contained in 0.2-mm-thick glass capillaries (Vitro Dynamics). The particles were first allowed to settle to the bottom of their containers, after which the measurement was performed on the sediment. This method was used to prevent a return of fluorescence during the measurement, which can result from particle diffusion or from convections generated by the large energy input.

3. Results and Discussion

A. Preparation. Particle radii obtained from the scattering curves are presented in Table 2 together with the radii and polydispersities obtained from the electron micrographs in Figure 1. The occurrence of deep minima in the angular dependence of the scattering indicated a low particle polydispersity. Only in system F6 was the minimum somewhat shallower, indicating some polydispersity. This is confirmed by the electron micrographs. System F6 also contains several larger particles that appear to have formed by the aggregation of two or three particles during the growth process. Radii obtained with TEM are about 11% smaller than those measured with SLS. This is a common phenomenon attributed to shrinkage of particles in the TEM vacuum chamber. This should not affect the values for the polydispersity, however. We find a polydispersity of about 6% which does not depend on the amount of dye in the particles, except for a sudden large increase in system F6.

Data on system F7 are not included in Table 2 because a stable colloid did not form in this sample. Instead, an orange precipitate consisting of large flocs was obtained. Incorporation of APS in the particles lowers the particles' stability because the basic amino groups add positive surface charges (R-NH_3^+) that partly compensate the negative charges (Si-O^-) on a normal silica surface (above $\text{pH} \sim 2$). Indeed, it has been shown in ref 8 that hybrid particles formed from APS/TES mixtures have a considerably lower surface charge than similar particles formed from TES alone. All other reactions formed stable colloids. System F6, however, was only marginally stable in DMF but completely stable in ethanol/ammonia because of the higher pH, which imparts a larger negative charge than DMF. These particles slowly aggregated over the course of several minutes and then settled rapidly. They could easily be resuspended by shaking. The effect of FITC would be to improve the stability because of the carboxylic acid group, but its effect should be much smaller because there is an excess of APS in the reaction.

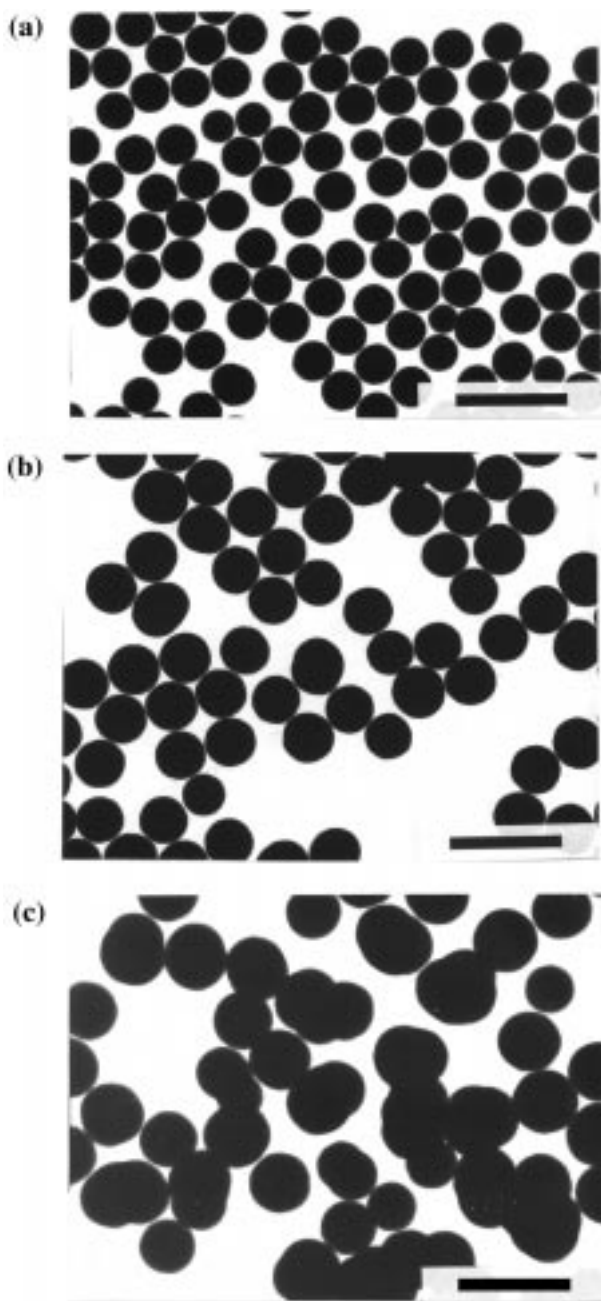


Figure 1. Electron micrographs of systems (a) F1, (b) F5, and (c) F6. In going from F1 to F5 the particles grow in size, but remain spherical and of equal polydispersity. System F6 shows signs of particle aggregation during growth. Scale bars are 1 μm .

From the data in Table 2 it is seen that the addition of a larger amount of APS–FITC to the reaction mixture of the silica synthesis leads to a slightly larger particle radius. This cannot be explained by the increasing volume of APS inside the particles. Even in F6 the APS/TES molar ratio is only 0.064. Although APS causes a slight decrease in particle density,⁸ this change is much too small to explain the increase in size. Instead, it is more likely that the size increase is again related to a lowering of the particle surface charge by the incorporation of APS. The reason is as follows: it is known that early in the reaction an aggregation occurs of siloxane oligomers that are not yet colloidally stable.^{25,26} Subsequent growth proceeds by monomer addition. The aggregation process stops when the oligomers become large enough to be stable colloidal particles, at which point the number of particles becomes fixed. Thus, the number of particles is determined by the stability of the

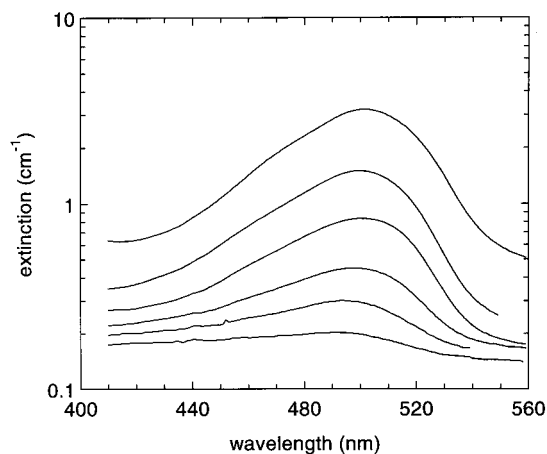


Figure 2. Absorption spectra of the FITC-labeled silica spheres in DMF. From lower to upper curve, systems F1–F6.

initial oligomers, which is lower when more APS is present. A smaller number of primary particles means that they will eventually grow out to larger particles. This is seen in Table 2.

The appearance of the particles varied gradually from yellow to deep orange going from F1 to F6. The labeling efficiencies, shown in Table 2, are given as the percentage of FITC molecules used in the synthesis that were detected by spectrophotometry after dissolution of the particles. The efficiency increases as the amount of labeling is increased, but remains relatively low. In line with this trend, Van Blaaderen et al.⁸ reported a larger fraction of incorporated APS of 37% (without FITC) starting from an equimolar APS/TES mixture. However, one would at first expect the opposite: lower efficiency at higher APS concentration. We are not certain of the cause of the increase. It may involve slow dissociation of the bond between APS and FITC in the ethanol/ammonia mixture. If NH_3 molecules could compete with the amino group of APS in the coupling reaction with FITC, then the relative number of surviving APS–FITC would increase with the amount of added APS–FITC. It would also explain why the labeling efficiencies are so low.

Although labeling efficiencies are only around 10%, effective dye concentrations inside the silica can be quite high. These are indicated in Table 2 as molar concentrations, assuming a typical silica density of 2.0 g/cm^3 . Also shown is the average distance between dye molecules in the particles, defined as

$$R = c^{-1/3} \quad (2)$$

where c is the number of molecules per unit volume. These values are on the order of the critical Förster distance for energy transfer, which is about 5.0 nm for fluorescein.²⁷ Therefore, quenching effects may be expected in our colloids.

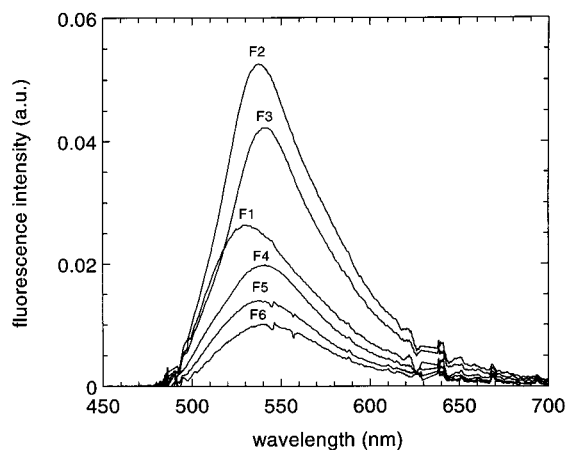
B. Spectroscopic Measurements. All FITC-labeled stock dispersions contained an equal concentration of silica, allowing direct comparison. The particle size and the refractive index difference between particles (1.45) and solvent (1.43) were chosen to be small in order to exclude strong scattering effects on absorption and fluorescence properties. The refractive index of the particles was determined by titrating DMF to a dispersion of particles in glycerol (index = 1.475) until the transmission (at 578 nm) was maximized in the optical match point. The refractive index of the matching fluid gave values of 1.450 ± 0.001 for all systems.

Absorption spectra of systems F1 to F6 are shown in Figure 2. The nonzero baselines are due to extinction resulting from some scattering. The absorption maximum (λ_{abs}) is seen to shift

TABLE 3: Spectroscopic Properties of FITC-Labeled Silica Spheres^a

system	λ_{abs} (nm)	λ_{em} (nm)	τ_1 (ns)	τ_2 (ns)	a_1/a_2	$\langle\tau\rangle$ (ns)	$I/I_0(10\text{ J})$
F1	491	531	1.1	3.93	0.45	3.69	0.52
F2	494	537	1.6	3.79	0.47	3.47	0.54
F3	497	541	1.2	3.28	1.09	2.75	0.65
F4	500	541				2.04	0.77
F5	500	540				2.02	0.80
F6	501	541				1.44	0.81

^a λ_{abs} and λ_{em} are the absorption and emission maxima, τ_1 and τ_2 are the fast and slow time scales in a double-exponential fit to the decay curves, a_1/a_2 is the ratio of their amplitudes, $\langle\tau\rangle$ is the average decay time, and $I/I_0(10\text{ J})$ is the fraction of fluorescence left after bleaching with 10 J of 488 nm light.

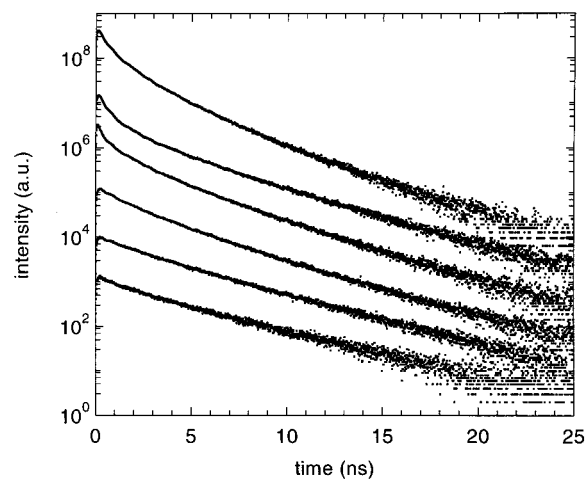
**Figure 3.** Fluorescence spectra (measured in backscattering geometry) of FITC-labeled silica spheres in DMF. Samples are as indicated.

to longer wavelengths as the particles' dye content is increased. The shift is 10 nm in going from F1 to F6, but is already largely completed at F4 (see Table 3). A small shoulder can be seen on the short-wavelength side of the absorption peak. This is a usual phenomenon in absorption spectra of FITC, both in solution and when bound to proteins.^{27,28} No evidence is found for an FITC dimer absorption peak.

The fluorescence spectra are plotted in Figure 3. Fluorescence maxima (λ_{em}) are given in Table 3. As expected from the absorption spectra, a red shift of about 10 nm occurs here as well upon increasing the dye content. Again the red shift is completed at system F4. The Stokes shift, the difference between absorption and fluorescence maxima, remains constant at 40 nm.

Red shifts may be caused by changes in the environment of dye molecules, such as changes in polarity or polarizability. The silica matrix is not expected to change much upon increasing the dye concentration, but the number of dye molecules that are in each others vicinity increases. This leads to interactions between neighboring molecules, which lowers their excited state energy and produces a red shift in the spectra. For example, in clay minerals an increase of adsorption of rhodamine 6G molecules was seen to lead to a similar red shift.²⁹ In our experiments these interactions also lead to significant self-quenching, which can be seen from the strong decrease in fluorescent intensity going from F3 to F6. Although a quantitative comparison of fluorescent intensities in Figure 3 is complicated by such factors as differences in scattering and strength of absorption, self-quenching is clearly evident from these spectra.

Strictly, we cannot exclude the possibility that part of the red shift in the fluorescence is caused by the inner filter effect: fluorescence on the blue side of the emission spectrum can be

**Figure 4.** Fluorescence decay curves. The curves have been offset for clarity. From lower to upper curve, F1 through F6.

suppressed by reabsorption due to overlap with the absorption spectrum. However, by measuring the fluorescence in reflection, we minimized the light path through the sample so that the inner filter effect should not be very strong. In addition, the absorption spectra show almost exactly the same trends, making it unlikely that the fluorescence spectra suffer from too much inner filtering.

It was verified that the fluorescence spectra did not depend appreciably on the wavelength used for excitation; excitation at 458, 476.5, and 488 nm gave identical spectra.

If the concentration-dependent red shift in the absorption and fluorescence spectra is the result of self-quenching due to interactions between close pairs of dye molecules, this red shift should be accompanied by a reduction of the fluorescence lifetimes. This is because a high probability of energy transfer between dye molecules shortens the time that molecules remain in their excited state. If quenching were due only to the formation of nonfluorescent dimers, then no change in lifetime would be expected, because these dimers do not contribute to the signal. Fluorescence decay curves are shown in Figure 4. Clearly, the concentration effect gives rise to a growing component with a very short lifetime.

Decay curves of the three most lightly labeled systems could be fitted well with a double-exponential curve, but not with a single exponent. The corresponding lifetimes (τ_1 and τ_2) and their relative amplitude (a_1/a_2) are given in Table 3. The longest lifetime is close to the $\tau_0 = 3.8\text{ ns}$ expected for a free FITC molecule.³⁰ It probably corresponds to single FITC molecules in silica. This lifetime decreases somewhat with increasing dye concentration, and its amplitude relative to the fast component of $\sim 1\text{ ns}$ becomes smaller. The fast component must be due to effects of rapid energy transfer between molecules. Decay curves of systems F4 to F6 could not be fitted satisfactorily to double exponentials and, indeed, seemed to possess a broad spectrum of lifetimes. In order to have a measure of the rate of decay, the average decay time $\langle\tau\rangle$ was determined by numerical integration of the decay curves (Table 3). It becomes rapidly smaller at higher dye contents, again indicating the appearance of faster decay modes.

We can estimate the rate of energy transfer $n_{\text{D}\rightarrow\text{A}}$ between donor and acceptor molecules by using the following expression by Förster:³¹

$$n_{\text{D}\rightarrow\text{A}} = \frac{1}{\tau_0} \left(\frac{R_0}{R} \right)^6 \quad (3)$$

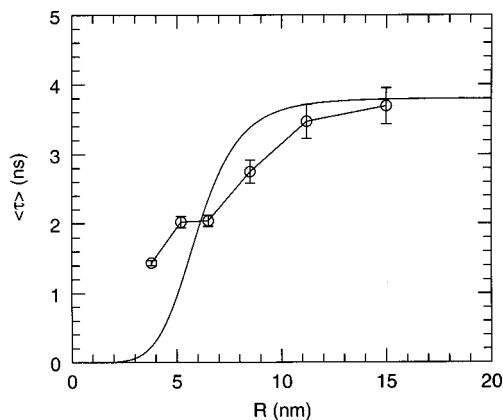


Figure 5. Average decay time as a function of the average intermolecular distance of FITC molecules. The full line is eq 4 with $R = 6$ nm and $\tau_0 = 3.8$ ns.

Here, R is the distance between donor and acceptor, and R_0 is the critical Förster distance—the distance at which 50% of the donors are deactivated by resonant energy transfer. Using the values $\tau_0 = 3.8$ ns³⁰ and $R_0 = 5.0$ nm,³¹ we expect transfer times $1/n_{D \rightarrow A}$ should be in the range of 0.7 ns for sample F6 to 2.8 μ s for sample F1. The dependence of the average decay time on the intermolecular distance should then be given by

$$\frac{1}{\langle \tau \rangle} = \frac{1}{\tau_0} + n_{D \rightarrow A} \quad (4)$$

In Figure 5 it is shown that a reasonable fit is obtained for $\tau_0 = 3.8$ ns and $R_0 = 6.0$ nm.

If there is energy transfer between molecules, one expects a decrease in fluorescence polarization with increased dye concentration. When a molecule is excited in a certain polarization direction, it will generally decay with the same polarization. However, when energy is transferred to acceptors with a different orientation than the donor molecule, the fluorescence becomes depolarized. Therefore, the time dependence of the fluorescence polarization anisotropy $r(t) = (I_{\parallel} - I_{\perp}) / (I_{\parallel} + 2I_{\perp})$ should provide information on the energy transfer process. However, the anisotropy showed instantaneous and complete depolarization at all dye concentrations. Thus, it is possible that the FITC molecules have a large amount of orientational freedom for rotation in the silica matrix, which does not allow observation of depolarization due to energy transfer.

We attempted to describe the fluorescence decay curves by three different models: quenching of excitations at the sphere's surface, a fractal distribution of dye molecules, and mutual annihilation of excitations.

In the first model, the excitations migrate diffusively through the sphere but are completely quenched when they reach the surface. Assuming an initially homogeneous distribution $u(\mathbf{r}, t)$ of excited molecules, the decay is described by the diffusion equation in spherical coordinates:

$$\frac{\partial u(r, t)}{\partial t} = D \left[\frac{\partial^2 u}{\partial r^2} + \frac{2}{r} \frac{\partial u}{\partial r} \right] - \frac{1}{\tau_0} u \quad (5)$$

$$u(R_S, t) = 0, u(r, 0) = u_0$$

Here, D is the effective diffusion coefficient, which is proportional to the transfer rate constant $n_{D \rightarrow A}$ and R_S is the radius of the sphere. The solution of eq 5 is integrated over the sphere's

volume to obtain the observed fluorescence:

$$u(t) = u_0 \sum_{n=1}^{\infty} \frac{1}{\pi^2 n^2} \exp(-t/\tau_0 - n^2 \pi^2 D t / R_S^2) \quad (6)$$

This formula clearly shows the competition between the spontaneous decay and the eigenmodes of the diffusion equation which result from quenching at the surface. Only the lower modes contribute and are negligible at longer times. Unfortunately, eq 6 does not describe the data very well. Also, the probability of an excitation reaching the sphere's surface is very small: using the energy transfer rates $n_{D \rightarrow A}$ calculated before, the excitation in sample F6 can migrate an average of only 5.5 steps of $R = 3.8$ nm before it decays radiatively. Because $D = (1/6)n_{D \rightarrow A}R^2$, the radiative decay rate in the leading order term in eq 6 is 3 orders of magnitude larger than the surface quenching rate. This separation is even larger for the other samples. We conclude, therefore, that surface quenching does not play an important role in the quenching process.

We also tried to fit the decay curves to a model of Klafter and Blumen^{32,33} describing the decay of an excited donor in the presence of acceptors, which are randomly distributed on a fractal of Hausdorff dimension d :

$$u(t) = u_0 \exp\{-t/\tau_0 - P(t/\tau_0)^{d/s}\} \quad (7)$$

with s the order of the molecular interaction ($s = 6$ for the usual Förster dipole–dipole mechanism) and P a fitting constant which should be proportional to the acceptor concentration. For integral dimensions, eq 7 reduces to the familiar results of Förster.³⁴ Equation 7 is known to work very well, giving d 's of usually roughly between 1.5 and 3.^{32,33,35} Although it does fit our data quite well, the dimension d takes on unrealistically low values between 0.3 and 1.5.

An alternative model could be to assume quenching by annihilation of excitations (singlet–singlet annihilation). In a system where rapid migration homogenizes the density of the excitations, the corresponding rate equation is

$$\frac{du(t)}{dt} = -\kappa u^2(t) - \frac{1}{\tau_0} u(t) \quad (8)$$

where κ is the rate constant of the second-order process. Solving this equation results in

$$\frac{1}{u(t)} = \left(\kappa \tau_0 + \frac{1}{u_0} \right) e^{t/\tau_0} - \kappa \tau_0 \quad (9)$$

If we fit this to our measurements on sample F6 (Figure 6, inset), we obtain a reasonable fit for $\tau_0 = 3.4$ ns and $\kappa = 2.3 \pm 0.3$ ns⁻¹. Thus, the coefficient of the second-order process is an order of magnitude greater than that of the first-order process. If this model describes the situation well, then the form of the decay curve should depend strongly on the initial excitation density u_0 . If u_0 is lowered, then the probability that two excitations meet is lowered and the decay curve should look more like a single-exponential process. We tested this by decreasing the excitation intensity by factors of 2 and 6, respectively (Figure 6). The resulting decay curves, however, did not change at all, making singlet–singlet annihilation an unlikely explanation. Alternatively, intensity-independent decay can sometimes be produced by singlet–triplet annihilation. Because triplet states are efficient quenchers and are long-lived (longer than our pulse separation), they could build up from pulse to pulse until a steady state is reached.³⁷ However, the

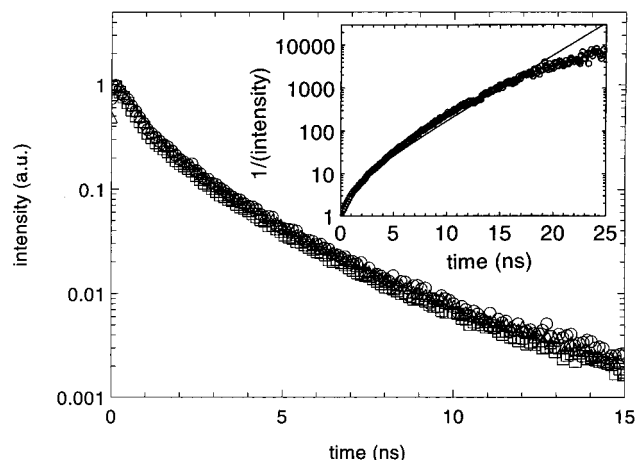


Figure 6. Decay curve of sample 6 (squares) and the influence of lowering the excitation intensity by a factor of 2 (triangles) and 6 (circles). The inset shows a fit of the excitation annihilation model eq 9 to these data.

intensity in our experiments was far too low to create enough triplets for such a process: we have at most 2×10^7 photons/pulse, whereas the number of spheres in the beam is $\sim 10^7$. Thus, there cannot be more than a few excitations per particle, of which only a small fraction ($\sim 1/1000$) are triplets.

Thus, none of these quite diverse quenching models describes the data very well. Because they all assume a homogeneous distribution of FITC molecules, this could be an indication that the distribution is not homogeneous. It cannot be excluded that the molecules have a tendency to be incorporated into the spheres in the form of clusters.

We can exclude Mie resonances and cooperative effects between different spheres due to scattering, such as are found in ref 14. In our case the refractive index difference between the spheres and the solvent was much too small. As an extra test we measured the decay curves of spheres suspended in water, where the index difference is much larger. Although care had to be taken to prevent excessive leaching of the dye due to hydrolysis of the outer layers of the silica spheres, it could be shown that the decay was the same.

Finally, we show that concentration effects in the FITC-labeled silica spheres have a clear effect on the dye's photostability. We shall refer to the decay of the emitted fluorescence as a function of exposure to the exciting intensity (at 488 nm) as the bleachcurve. These curves are shown in Figure 7. Even at the lowest dye concentration, the bleachcurves do not show the single exponential decay that would be expected for a simple first-order process. A fast bleaching mode during the first few seconds is followed by a much slower one. Whereas FITC solutions are known to show single exponential bleaching (or fading), FITC-labeled biological samples always bleach in a nonsingle exponential fashion. The kinetics of this process has recently been studied.^{22,23} The nonsingle exponential behavior was attributed to a variation in the microenvironment of the dye molecules, such as the availability of oxygen,²² or to interactions between excited dye molecules.²³ A variation in environment seems a likely explanation in the case of our amorphous silica particles, but we will now argue that molecular interactions also play an important role.

If dye molecules are completely independent, the bleachcurves will not depend on concentration. After all, doubling the concentration will then also double the number of bleached dye molecules. Therefore, the fluorescence relative to its initial value should be the same in both cases. This appears to be the

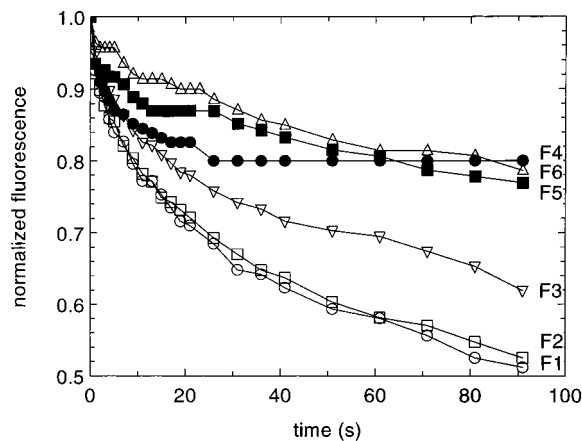


Figure 7. Bleach curves showing the relative decrease of the fluorescence as a function of the duration of irradiation with 488 nm light of 0.10 W.

case in silicas F1 and F2, yet these systems already show nonsingle exponential bleaching. In the more heavily labeled systems the rate of photobleaching is considerably smaller, but reaches almost equal long-time levels in systems F4, F5, and F6. To quantify this, we show in Table 3 the percentage of fluorescence left after exposure to 10 J of 488 nm light, $I/I_0(10 \text{ J})$. When compared to laser dyes such as Rhodamine 6G,⁵ our fluorescein samples bleach many times faster. But our data also show that the photostability increases when the dye content of the particles is increased. This increase takes place in the same concentration range (F1–F4) as the spectral shifts. It is unlikely that this effect is caused by the reduction of the absorption coefficient at 488 nm resulting from the red shift of the absorption peak. This shift should lead to a proportional reduction of the fluorescence and is therefore removed by normalization on the initial fluorescence.

A reduction in the rate of photobleaching upon increasing the dye concentration has not been reported before. However, it has been shown experimentally^{22,38} that the presence of efficient acceptor molecules (which were different from the FITC donor molecules) considerably decreases the rate of photobleaching. By transfer of energy from donors to acceptors, the excited state, in which molecules are sensitive to bleaching, is depopulated more quickly, making bleaching a less probable process. The effects noted in the present work point to a similar mechanism. In the case of self-quenching, the donors are identical to the acceptors. Depopulation of the excited state takes place by energy migration to sites where radiationless decay occurs.

Although this process seems to be the most likely explanation for the increased photostability, other effects could also play a role. For example, if it is assumed that bleached FITC molecules are less efficient quenchers of fluorescence than FITC molecules themselves, then an increase in fluorescence is expected when the sample is partly bleached. This would be interpreted as an increased photostability. However, it is impossible to establish the likelihood of this explanation since not much is known about the nature and properties of the bleaching products of FITC (or those of other dyes).

4. Conclusions

A series of colloidal suspensions was prepared from monodisperse silica spheres laced with increasing amounts of the fluorescent dye FITC. Stable colloids could be prepared with a dye concentration inside the silica of up to 0.03 M. Labeling

efficiencies were in the range of 6.6% to 13%. Strong effects of interactions between the dye molecules were found, leading to excitation quenching. A red shift of 10 nm occurred in the absorption and fluorescence spectra upon traversing the concentration range 0.5–5 mM (inside silica). Simultaneously, the fluorescence lifetime and the rate of photobleaching of the dye were strongly reduced, pointing to energy transfer taking place between dye molecules. The fluorescence decay curves could not be described satisfactorily with models involving second-order processes, surface quenching, or a fractal distribution of dye molecules. A possible explanation is that the FITC molecules are not distributed homogeneously, but form clusters with intermolecular distances of less than the Förster distance. Second-order effects such as excitation annihilation then explain why quenching effects are observed already at low dye concentrations.

These findings have consequences for the use of FITC-labeled silica particles with different experimental techniques. In applications such as particle imaging in colloidal dispersions with fluorescence microscopy, or the preparation of new optical materials in lasers and filters, a low level of bleaching is desirable. Particle dye contents should then be optimal at around 5 mM. At higher concentrations the high fluorescence photostability remains, but the fluorescence yield decreases too much by self-quenching. For measurements of particle mobility with fluorescence recovery after photobleaching, a high fluorescence yield should ideally be combined with a high level of bleaching. Our results indicate that dye concentrations of around 0.5–1 mM are optimal to achieve this level. These low concentrations are also preferred when energy transfer effects within the spheres are undesirable altogether, such as in the study of multiple scattering effects.

Acknowledgment. This work is part of the research program of the Foundation for Fundamental Research on Matter (FOM) with financial support from the Netherlands Organization for Scientific Research (NWO).

References and Notes

- See, e.g.: (a) Reisfeld, R.; Yariv, E.; Minti, H. *Opt. Mater.* **1997**, *8*, 31. (b) Costela, A.; Garcia-Moreno, I.; Figueira, J. M.; Amat-Guerri, F.; Barroso, J.; Sastre, R. *Opt. Commun.* **1996**, *130*, 44, and references therein.
- See, e.g.: Bentivegna, F.; Canva, M.; Georges, P.; Brun, A.; Chaput, F.; Malier, L.; Boilot, J. P. *Appl. Phys. Lett.* **1993**, *62*, 1721.
- See, e.g.: Canva, M.; Le Saux, G.; Georges, P.; Brun, A.; Chaput, F.; Boilot, J. P. *Opt. Lett.* **1992**, *17*, 218.
- See, e.g.: Reisfeld, R.; Zusman, R.; Cohen, Y.; Eyal, M. *Chem. Phys. Lett.* **1988**, *147*, 142.
- (a) Avnir, D.; Kaufman, V. R.; Reisfeld, R. *J. Non-Cryst. Solids* **1985**, *74*, 395. (b) McKiernan, J. M.; Yamanaka, S. A.; Dunn, B.; Zink, J. I. *J. Phys. Chem.* **1990**, *94*, 5652.
- See e.g.: Wehry, E. L.; Rogers, L. B. In *Fluorescence and Phosphorescence Analysis*; Hercules, D. M., Ed.; Interscience: New York, 1966; pp 81–149.
- van Blaaderen, A.; Vrij, A. *Langmuir* **1992**, *8*, 2921.
- van Blaaderen, A.; Vrij, A. *J. Colloid Interface Sci.* **1993**, *156*, 1.
- Bowden, C. M.; Dowling, J. P.; Everitt, H. O. (Eds.) Development and applications of materials exhibiting photonic band gaps. *J. Opt. Soc. Am. B* **1993**, *10*, 280.
- Yablonovitch, E. *Phys. Rev. Lett.* **1987**, *58*, 2059.
- (a) Vos, W. L.; Sprik, R.; van Blaaderen, A.; Imhof, A.; Lagendijk, A.; Wegdam, G. H. *Phys. Rev. B* **1996**, *53*, 16231; (E) **1997**, *55*, 1903. Vos, W. L.; Megens, M.; van Kats, C. M.; Bösecke, P. *J. Phys.: Condens. Matter* **1996**, *8*, 9503.
- Martorell, J.; Lawandy, N. M. *Phys. Rev. Lett.* **1990**, *65*, 1877.
- (a) Tong, B. Y.; John, P. K.; Zhu, Y.-t.; Liu, Y. S.; Wong, S. K.; Ware, W. R. *J. Opt. Soc. Am. B* **1993**, *10*, 356. (b) Lawandy, N. M. *J. Opt. Soc. Am. B* **1993**, *10*, 2144.
- Tomita, M.; Ohosumi, K.; Ikari, H. *Phys. Rev. B* **1994**, *50*, 10369.
- Wiersma, D. S.; Lagendijk, A. *Phys. World* **1997**, *10*, 33.
- See, e.g.: (a) Eversole, J. D.; Lin, H. B.; Huston, A. L.; Campillo, A. J.; Leung, P. T.; Liu, S. Y.; Young, K. *J. Opt. Soc. Am. B* **1993**, *10*, 1955. (b) Popp, J.; Fields, M. H.; Chang, R. K. *Opt. Lett.* **1997**, *22*, 1296 and references therein.
- Sandoghdar, V.; Treussart, F.; Hare, J.; Lefèvre-Seguin, V.; Raimond, J. M.; Haroche, S. *Phys. Rev. A* **1996**, *54*, R1777.
- Imhof, A.; van Blaaderen, A.; Maret, G.; Mellema, J.; Dhont, J. K. G. *J. Chem. Phys.* **1994**, *100*, 2170.
- (a) van Blaaderen, A.; Imhof, A.; Hage, W.; Vrij, A. *Langmuir* **1992**, *8*, 1514. (b) van Blaaderen, A.; Wiltzius, P. *Science* **1995**, *270*, 1177.
- Verhaegh, N. A. M.; van Blaaderen, A. *Langmuir* **1994**, *10*, 1427.
- Stöber, W.; Fink, A.; Bohn, E. *J. Colloid Interface Sci.* **1968**, *26*, 62.
- Young, R. M.; Arnette, J. K.; Roess, D. A.; Barisas, B. G. *Biophys. J.* **1994**, *67*, 881.
- Song, L. L.; Hennink, E. J.; Young, I. T.; Tanke, H. J. *Biophys. J.* **1995**, *68*, 2588.
- Böhren, C. F.; Huffman, D. R. *Absorption and Scattering of Light by Small Particles*; John Wiley & Sons: New York, 1983.
- Bogush, G. H.; Zukoski IV, C. F. *J. Colloid Interface Sci.* **1991**, *142*, 1.
- van Blaaderen, A.; van Geest, J.; Vrij, A. *J. Colloid Interface Sci.* **1992**, *154*, 481.
- Lakowicz, J. R. *Principles of Fluorescence Spectroscopy*; Plenum Press: New York, 1983.
- Nairn, R. C. *Fluorescent Protein Tracing*, 4th ed.; Churchill Livingstone: Edinburgh, 1976.
- Grauer, Z.; Avnir, D.; Yariv, S. *Can. J. Chem.* **1984**, *62*, 1889.
- Haugland, R. P.; Larison, K. D. (Eds.) *Handbook of Fluorescent Probes and Research Chemicals*; Molecular Probes Inc.: 1996.
- Förster, Th. *Discuss. Faraday Soc.* **1959**, *27*, 7.
- Klafter, J.; Blumen, A. *J. Chem. Phys.* **1984**, *80*, 875.
- Levitz, P.; Drake, J. M.; Klafter, J. *J. Chem. Phys.* **1988**, *89*, 5224.
- (a) Förster, Th. *Ann. Phys. (Leipzig)* **1948**, *2*, 55. (b) Förster, Th. *Z. Naturforsch.* **1949**, *4A*, 321.
- Nakashima, K.; Duhamel, J.; Winnik, M. A. *J. Phys. Chem.* **1993**, *97*, 10702.
- Rojanski, D.; Huppert, D.; Bale, H. D.; Dacai, X.; Schmidt, P. W.; Farin, D.; Seri-Levy, A.; Avnir, D. *Phys. Rev. Lett.* **1986**, *56*, 2505.
- Shapiro, S. L. *Ultrashort Light Pulses: Picosecond Techniques and Applications*, 2nd ed.; Springer Verlag: Berlin, 1984; p 343.
- Jovin, T. M.; Arndt-Jovin, D. J. FRET Microscopy: Digital imaging of fluorescence resonance energy transfer. Application in cell biology. In *Cell Structure and Function by Microspectrofluorometry*; Kohen, E., Hirschberg, J. G., Eds.; Academic Press: London, 1989; pp 99–117.